JGR Atmospheres

RESEARCH ARTICLE
10.1029/2024JD040811

A Single Compartment Relaxed Eddy Accumulation Method

T. Banerjee[1], G. G. Katul[2], E. Zahn[3], N. L. Dias[4], and E. Bou-Zeid[3]

[1]Department of Civil and Environmental Engineering, University of California, Irvine, CA, USA, [2]Department of Civil and Environmental Engineering, Duke University, Durham, NC, USA, [3]Department of Civil and Environmental Engineering, Princeton University, Princeton, NJ, USA, [4]Departamento de Engenharia Ambiental, Universidade Federal do Paraná, Paraná, Brazil

Key Points:

- Relaxed eddy accumulation (REA) is used to estimate turbulent fluxes of numerous chemical species
- The original REA relies on sampling concentrations in two compartments
- A single-compartment REA is proposed with no loss in accuracy

Correspondence to:

T. Banerjee,
tirthab@uci.edu

Citation:

Banerjee, T., Katul, G. G., Zahn, E., Dias, N. L., & Bou-Zeid, E. (2024). A single compartment relaxed eddy accumulation method. *Journal of Geophysical Research: Atmospheres*, *129*, e2024JD040811. https://doi.org/10.1029/2024JD040811

Received 26 JAN 2024
Accepted 22 SEP 2024

Abstract The relaxed eddy accumulation (REA) method is a widely-known technique that measures turbulent fluxes of scalar quantities. The REA technique has been used to measure turbulent fluxes of various compounds, such as methane, ethene, propene, butene, isoprene, nitrous oxides, ozone, and others. The REA method requires the accumulation of scalar concentrations in two separate compartments that conditionally sample updrafts and downdraft events. It is demonstrated here that the assumptions behind the conventional or two-compartment REA approach allow for one-compartment sampling, therefore called a one compartment or 1-C-REA approach, thereby expanding its operational utility. The one-compartment sampling method is tested across various land cover types and atmospheric stability conditions, and it is found that the one-compartment REA can provide results comparable to those determined from conventional two-compartment REA. This finding enables rapid expansion and practical utility of REA in studies of surface-atmosphere exchanges, interactions, and feedbacks.

Plain Language Summary Estimates of emission inventory of chemical compounds from the biosphere remain an indispensable tool in air quality and climate science research. Such inventory requires the measurements of the number of molecules flowing from the biosphere to the atmosphere, or vice-versa, per unit ground area per unit time. What makes these measurements challenging is that such molecules are being transported rapidly by gusts and swirling (i.e., turbulent) motion in the atmosphere. In theory, this vertical exchange can be measured by a rapidly sampled covariance between vertical velocity and concentration variations. The main drawback is that such covariance requires rapid concentration measurements that are difficult to conduct for a large number of chemical species, although it is standard practice and easier to obtain for carbon dioxide, water vapor, and air temperature. The work here offers an alternative and efficient approach that necessitates measuring the accumulation of molecules in a single compartment, supplemented by knowledge of the velocity statistics. Both velocity and accumulated concentration measurements can be conducted with available instrumentation. Thus, the work here offers a blueprint for efficient sampling of emission rates across the biosphere-atmosphere interface that can be deployed in upcoming experiments.

1. Introduction

The relaxed eddy accumulation (REA) method is used to estimate turbulent scalar fluxes when fast-response sensors for measuring vertical velocity fluctuations are available (typically from sonic anemometers) but only mean or accumulated concentration measurements can be conducted for the scalars. The premise behind estimating turbulent fluxes using a conditional sampling formulation was first conceived in the 1970s (Desjardins, 1977) but derived in its current form in the early 1990s (Businger & Oncley, 1990) as an alternative or supplement to eddy covariance (EC) techniques. The REA method gained popularity in atmospheric chemistry given the difficulty in measuring concentrations of many chemical compounds such as volatile organic compounds (VOC) at high frequency (Bowling et al., 1998; Dabberdt et al., 1993; Grelle & Keck, 2021; McInnes & Heilman, 2005; Olofsson et al., 2003; Oncley et al., 1993; Pattey et al., 1993). Several prototypes have already been proposed and built for terrestrial ecosystems (Arnts et al., 2013; B. Baker et al., 1999; Beverland et al., 1996; Nie et al., 1995; Sarkar et al., 2020) and air-sea exchanges (Brut et al., 2004; Dabberdt et al., 1993), but the methodology for computing turbulent fluxes remains the same across all REA systems and is given by

$$\overline{w'c'} = \beta\sigma_w\left(\overline{c^+} - \overline{c^-}\right), \tag{1}$$

where $\overline{w'c'}$ is the sought vertical turbulent flux of scalar c, w' is the turbulent vertical velocity, c' is the turbulent scalar concentration fluctuation, overline denotes time-averaging, β is a coefficient to be externally specified but assumed constant independent of surface cover or thermal stratification, $\sigma_w = \sqrt{\overline{w'^2}}$ is the vertical velocity standard deviation, $\overline{c^+}$ and $\overline{c^-}$ are mean concentrations that must be collected in two separate compartments: one for updraft events (i.e., $w' > 0$) and another for downdraft events (i.e., $w' < 0$). The advantages of the REA are evident as σ_w can be measured using standard sonic anemometers and $\overline{c^+}$ as well as $\overline{c^-}$ do not require any high-frequency measurements. For some trace gases and VOC, $\overline{c^+}$ and $\overline{c^-}$ can be measured by gas chromatography that is significantly expensive and requires specialized expertise. The REA is routinely used to measure fluxes of butene, ethene, isoprene, methane, nitrous oxides, and propene across many biomes (B. Baker et al., 1999; Darmais et al., 2000; Denmead, 2008; Desjardins et al., 2010; Pattey et al., 1999; Ren et al., 2011; Rhew et al., 2017; Velentini et al., 1997) along with nitrous acid (HONO) (von der Heyden et al., 2022; Zhang et al., 2012), terpenoid fluxes (Mochizuki et al., 2014), ammonia, and its volatilization from agricultural fields (Hensen et al., 2009; Meyers et al., 2006; Zhu et al., 2000), herbicides volatilization (Pattey et al., 1995), fluxes of several carbon-based compounds such as carbonyl sulfide and carbon disulfide (Xu et al., 2002), halocarbon (Hornsby et al., 2009), and dimethyl sulfide in air-sea exchanges (Held et al., 2008; H. Zemmelink et al., 2002; H. J. Zemmelink et al., 2004). Moreover, the REA concept has been extended to measure aerosols and ultrafine particle fluxes (Gaman et al., 2004; Grönholm et al., 2007; Meskhidze et al., 2018; Pryor et al., 2007; Schery et al., 1998) and has been successfully used for estimating sediment-water exchanges in aquatic systems (Lemaire et al., 2017).

The REA method requires the specification of β that has also received significant attention over the last 30 years (Andreas et al., 1998; J. Baker et al., 1992; Gao, 1995; G. Katul et al., 1994; G. G. Katul et al., 1996; Milne et al., 1999; Zahn et al., 2016, 2023). Some studies report high variability in β (Ruppert et al., 2006) while others appear to suggest a near-constant value $\beta = 0.55$–0.59 for atmospheric conditions that are not too stably stratified (Ammann & Meixner, 2002; G. G. Katul et al., 1996; Tsai et al., 2012; Sakabe et al., 2014). This constant $\beta = 0.55$–0.59 was also reported across many sites including forests and agricultural sites (J. Baker et al., 1992; Gao, 1995; G. Katul et al., 1994; G. G. Katul et al., 1996), wetlands (Tsai et al., 2012), peatlands (G. Katul et al., 2018), among others. The invariance of β with respect to atmospheric stability conditions was also discussed (Zahn et al., 2023). Others report a $\beta = 0.6$ for stable atmospheric conditions and $\beta = 0.56$ for unstable conditions over a forest (Dias et al., 2023). Yet, other studies did show that scatter in β can be partially explained by variations in higher-order cumulants of the joint probability density function ($JPDF$) formed between w' and c' (G. Katul et al., 2018; Milne et al., 1999). These findings are suggestive that deviations in the $JPDF(w', c')$ from Gaussian, often attributed to large contributions in the outward-inward interaction terms (i.e., counter-flux motions) that weaken the turbulent fluxes, may be partially responsible for some of the scatter in β.

The work here explores the basic assumption of REA, which is the estimation of the correlation coefficient between w' and c' from updrafts $(w' > 0)$ and downdrafts $(w' < 0)$ using linear regression theory. It is shown that the linearity assumption that is inherent to the conventional or two-compartment REA (2C-REA) method invites the development of one-compartment measuring systems. This approach leads to an estimate of the scalar fluxes based on concentration accumulation in updrafts or downdrafts (but not necessarily both). As in the 2C-REA, the newly proposed approach requires an adjustment factor shown to be commensurate to adjustments in β from those derived for a Gaussian distribution. The approach, along with the inherent assumptions necessary to develop the one-compartment REA (1C-REA) approach is tested using measured time series of vertical velocity, longitudinal velocity, and air temperature collected over a variety of ecosystems spanning forests, grassland, soils, ice sheets, and lakes. The agreement between measured turbulent fluxes and predicted from a one-compartment model is encouraging but should be treated as a proof-of-concept.

2. Theory

Throughout, the mass exchange of a scalar c between an underlying surface and the atmosphere is presumed to be fully turbulent so that the vertical flux is given by

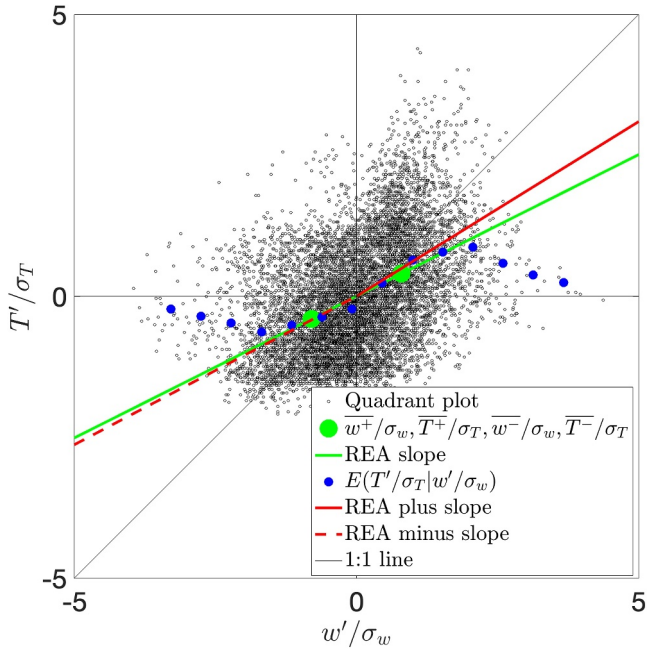

Figure 1. Conceptual representation of the relaxed eddy accumulation (REA) method. Black circles represent the quadrant plot of measured w'/σ_w and T'/σ_T from one of the 30-min runs over the pine canopy in the Duke forest. In this case, $\overline{w'T'} > 0$ and quadrants 1 (ejection) and 3 (sweeps) are the contributors to the turbulent flux while quadrants 2 (inward interaction) and 4 (outward interaction) oppose the turbulent flux and are known as "counter-flux." The solid black lines denote the axes and the one-to-one line. The green circles denote the coordinates of the points $(\overline{w^+}/\sigma_w, \overline{T^+}/\sigma_T)$, and $(\overline{w^-}/\sigma_w, \overline{T^-}/\sigma_T)$ in the quadrant plane. The green line connecting the green points is the slope used in the relaxed eddy estimation (REA) as stated in Equation 3. Blue circles show the empirically determined expected values of T'/σ_T, conditioned on binned values of w^+/σ_w and w^-/σ_w as a precursor to Equation 21. The solid red line represents the positive one-compartment REA slope and the dashed red line represents the negative one-compartment REA slope respectively as stated in Equation 21.

$$\overline{w'c'} = R_{wc}\sigma_w\sigma_c, \tag{2}$$

where w and c are, as before, the instantaneous vertical velocity and scalar concentrations, respectively. Primed quantities are deviations from their time-averaged states that are indicated by an overbar (i.e., $\overline{c'} = 0$, $\overline{w'} = 0$), $\sigma_c = \left(\overline{c'^2}\right)^{1/2}$ is the root-mean-squared scalar concentration fluctuations, and R_{wc} is the correlation coefficient between w' and c', which represents the efficiency of scalar transport. The traditional quadrant analysis (G. Katul et al., 2006) is used to classify turbulent motions that are to be conditionally sampled in the estimation of $\overline{w'c'}$ in REA formulations. These quadrants are formed in a $w' - c'$ plane with abscissa $x = w'/\sigma_w$ and ordinate $y = c'/\sigma_c$ as shown in Figure 1. When $\overline{w'c'} > 0$, ejection events ($w' > 0$, $c' > 0$) are associated with quadrant 1, and sweep events ($w' < 0, c' < 0$) are associated with quadrant 3, which are called "co-flux" motions. On the other hand, inward ($w' < 0, c' > 0$) (quadrant 2) and outward ($w' > 0, c' < 0$) interaction events (quadrant 4) are labeled as "counter-flux" because they act to reduce the net $\overline{w'c'}$. Conversely, when $\overline{w'c'} < 0$, ejection events ($w' > 0$, $c' < 0$) are associated with quadrant 4, sweep events ($w' < 0, c' > 0$) are associated with quadrant 2, inward ($w' < 0, c' < 0$) (quadrant 3) and outward ($w' > 0$, $c' > 0$) (quadrant 1) quadrants are now labeled as "counter-flux" because they still act to reduce the magnitude of the net $\overline{w'c'}$.

2.1. Review of the REA Method

From linear correlation analysis (to be elaborated upon later), the regression slope of $x = w'/\sigma_w$ (abscissa) against $y = c'/\sigma_c$ (ordinate) can be related to the correlation coefficient using

$$R_{wc} = \frac{\left(\overline{c^+} - \overline{c^-}\right)/\sigma_c}{\left(\overline{w^+} - \overline{w^-}\right)/\sigma_w}, \tag{3}$$

where, once again, $\overline{c^+}$ is the conditional average of scalar c instantaneously attributed to updrafts events $\left(w' > 0\right)$, and $\overline{c^-}$ is the conditional average of scalar c instantaneously attributed to downdrafts events $\left(w' < 0\right)$ as shown in Figure 1. When this estimate for R_{wc} is inserted into Equation 2, the 2C-REA method becomes

$$\overline{w'c'} = \left[\frac{\sigma_w}{\left(\overline{w^+} - \overline{w^-}\right)}\right]\sigma_w\left(\overline{c^+} - \overline{c^-}\right). \tag{4}$$

The estimates of R_{wc} from the data and the regression slope using Equation 3 are featured in Figure 1. The figure is suggestive that R_{wc} can be reliably estimated from only two points (large green dots in the figure) as necessary for the 2C-REA since the velocity fluctuations are obtained after de-meaning the time series so that the mean of the fluctuations is always zero, and the scatterplot must be centered around the (0, 0) point.

The mathematical form of Equation 4 may also offer an explanation as to why β in Equation 1 appears constant across studies. To illustrate, consider a Gaussian distributed w' with a probability density function $PDF\left(w'\right)$ given by

$$PDF\left(w'\right) = \frac{1}{\sqrt{2\pi}\sigma_w}\exp\left(-\frac{w'^2}{2\sigma_w^2}\right). \tag{5}$$

Using this assumed $PDF(w')$, the w^+ points define a half-normal distribution and $\overline{w^+}$ can thus be determined as (J. Baker et al., 1992; G. Katul et al., 2018)

$$\overline{w^+} = \frac{\int_0^\infty w' PDF(w') dw'}{\int_0^\infty PDF(w') dw'} = \frac{\left(\sigma_w/\sqrt{2\pi}\right)}{(1/2)}, \tag{6}$$

where the numerator denotes the ensemble mean of $w' > 0$ and the denominator denotes the fraction of time $w' > 0$ (i.e., $= 1/2$). Likewise, $\overline{w^-} = -2\sigma_w/\sqrt{2\pi}$. Hence, a coefficient β_g associated with a Gaussian $PDF(w')$ can now be introduced to further simplify the REA formulation as

$$\beta_g = \frac{\sigma_w}{\left(\overline{w^+} - \overline{w^-}\right)} = \frac{\sqrt{2\pi}}{4}, \tag{7}$$

which is a constant independent of the flow and the scalar concentration statistics. However, this value of $\beta_g = 0.63$ appears higher than those reported in a number of experiments ($\beta = 0.55$–0.59) as reviewed elsewhere (G. G. Katul et al., 1996). This discrepancy of linear regression analysis to estimate R_{wc} from Equation 3 has led some to propose an operational REA model that simply replaces Equation 4 with Equation 1 while treating β as an externally supplied coefficient, usually a constant smaller than β_g. This failure along with $\beta/\beta_g \leq 1$ is most evident when the $JPDF(w', c')$ is non-Gaussian and counter-flux events occur in significant fraction during the sampling duration.

The quantification of non-Gaussian $JPDF(w', c')$ on the interaction between w' and c' can be evaluated using a Shannon information entropy (Shannon, 1948) or level of mutual dependence given by Paluš and Novotná (1994)

$$I(w', c') = \iint JPDF(w', c') \ln\left(\frac{JPDF(w', c')}{PDF(w') PDF(c')}\right) dw' dc', \tag{8}$$

where $I(w', c')$ is defined as a mutual information content between w' and c'. To normalize this measure to be bounded between [0, 1], a transformation

$$\Lambda = \sqrt{1 - \exp\left[-2I(w', c')\right]} \tag{9}$$

can be used, which can also be labeled as a generalized correlation coefficient (Tsonis, 2001). When the $JPDF(w', c')$ is Gaussian characterized by a correlation coefficient R_{wc}, $I_G(w', c') = (-1/2)\ln(1 - R_{wc}^2)$ and $\Lambda_G = |R_{wc}|$. This means that when the $JPDF(w', c')$ is Gaussian, the generalized correlation coefficient reduces to the linear correlation coefficient (Tsonis, 2001). Thus, the absolute difference between Λ and $|R_{wc}|$ (or $\Lambda_{I_G} = |R_{wc}|$) may be used to assess inadequacies of linear correlation models to capture interactive effects between w' and c' and link them to deviations from a Gaussian $JPDF(w', c')$. The absolute difference between Λ_I and $|R_{wc}|$ proved to be effective in analyzing the Mackey-Glass model (a non-linear time-delayed differential equation) where Λ_I is significant but $|R_{wc}|$ is not (Tsonis, 2001; Tsonis et al., 1994).

Tracking analytically these effects on β requires additional simplifications. A way forward is to employ fourth-order cumulant expansion methods (CEMs) and simplifications to them on the *PDF*s and *JPDF*s. It has been repeatedly demonstrated that CEMS describe the flow statistics well in the roughness sublayer above obstacles (Heisel et al., 2020), in the canopy sublayer above rods with varying rod densities (Poggi et al., 2004), in multiple forest types and across many stability regimes (Cava et al., 2006; Banerjee et al., 2017; G. Katul, Hsieh, Kuhn, et al., 1997), in sparse canopies on sloping terrain (Francone et al., 2012), in rod canopy on hills (Poggi & Katul, 2007), over bare soils and ice sheets (Fer et al., 2004; G. Katul et al., 2006), in many regions of smooth walled open channels (Nakagawa & Nezu, 1977), and in the inner and outer layers of rough-walled wind tunnel

experiments across many types of roughness elements (Heisel et al., 2020; Raupach, 1981). The utility of fourth-order CEM yields (Milne et al., 1999; G. Katul et al., 2018)

$$\beta_{CEM} = \frac{\frac{4}{9}\sqrt{\frac{\pi}{2}}}{1 + \frac{4}{27}\left(\frac{3}{4}M_{40} - \frac{M_{31}}{M_{11}}\right)}, \tag{10}$$

where $M_{ij} = \overline{w'^i c'^j}/\left(\sigma_w^i \sigma_c^j\right)$, thus $M_{40} = \overline{(w'/\sigma_w)^4}$ is the kurtosis or flatness factor (a measure of intermittency) of the vertical velocity fluctuations (i.e., the same for all scalars), $M_{31} = \overline{(w'/\sigma_w)^3 (c'/\sigma_c)}$ is related to the strength of the interaction between the asymmetry in w' and c' (and can vary across scalars), and $M_{11} = R_{wc} = \overline{(w'/\sigma_w)(c'/\sigma_c)}$ is, as before, the correlation coefficient. It is instructive to note that when

$$\frac{3}{4}M_{40} = \frac{M_{31}}{M_{11}}, \tag{11}$$

$\beta = (4/9)\sqrt{\pi/2} = 0.56$, which is smaller than $\beta_g = 0.63$ but closer to the empirically reported range between 0.55 and 0.59. A possible cause for the coordination between M_{40} and M_{31}/M_{11} needed to explain a constant $\beta = 0.56$ is proposed. For four arbitrary variables that are Gaussian distributed (a', b', c', and d'), the fourth moment is given by Monin and Yaglom (1971), Nakagawa and Nezu (1977)

$$\overline{a'b'c'd'} = \overline{a'b'}\ \overline{c'd'} + \overline{a'c'}\ \overline{b'd'} + \overline{a'd'}\ \overline{b'c'}. \tag{12}$$

Adopting this approximation for $\overline{w'w'w'c'}$ and expanding yields

$$\frac{M_{31}}{M_{11}} = \frac{\overline{w'w'w'c'}}{\overline{w'c'}}\frac{\sigma_w\sigma_c}{\sigma_w^3\sigma_c} = 3\frac{\overline{w'w'}\ \overline{w'c'}}{\overline{w'c'}}\frac{1}{\sigma_w^2} = 3. \tag{13}$$

Recalling that $M_{40} = 3$ for a Gaussian process results in direct equality between M_{40} (=3) and M_{31}/M_{11} (=3) when deviations from Gaussian distribution are small. The small imbalance between $(3/4)M_{40}$ and M_{31}/M_{11} in Equation 10 is necessary to recover β_g when the flow statistics are Gaussian. Under the assumption that $M_{40} = 3$ and $M_{31}/M_{11} = 3$ (i.e., Gaussian),

$$\beta_{CEM} = \frac{\frac{4}{9}\sqrt{\frac{\pi}{2}}}{1 + \frac{4\times3}{27}\left(\frac{3}{4} - 1\right)} = \frac{1}{2}\sqrt{\frac{\pi}{2}} = \beta_g. \tag{14}$$

The formulation in Equation 10 makes clear that the mechanisms deciding on whether $\beta_{CEM}/\beta_g < 1$ or $\beta_{CEM}/\beta_g > 1$ depend on how non-Gaussianity impacts M_{40} and M_{31}/M_{11}. As $M_{31}/M_{11} \to 0$ and $M_{40} > 4$ results in $\beta_{CEM} < 0.39$. Conversely, a near-Gaussian M_{40}(=3) and a larger than Gaussian M_{31}/M_{11} (=4) can lead to $\beta_{CEM} > 0.7$.

2.2. A One-Compartment REA (1C-REA)

As noted earlier, the conventional REA requires two compartments—one for accumulating scalar mass associated with updrafts and another associated with downdrafts. However, when enforcing the regression of $y = c'/\sigma_c$ against $x = w'/\sigma_w$ to pass through the origin $x = 0$, $y = 0$, two other slope estimates for R_{wc} can be introduced. These estimates form the basis of what is now labeled as one-compartment model. These two regression slopes, also shown in Figure 1, are now given as

$$R_{wc,+} = \frac{\overline{c^+}/\sigma_c}{\overline{w^+}/\sigma_w}; R_{wc,-} = \frac{\overline{c^-}/\sigma_c}{\overline{w^-}/\sigma_w}. \tag{15}$$

With these estimates, the single-compartment REA approach is

$$\overline{w'c'} = \left[\frac{\sigma_w}{\overline{w^+}}\right]\sigma_w(\overline{c^+}) = \left[\frac{\sigma_w}{\overline{w^-}}\right]\sigma_w(\overline{c^-}). \tag{16}$$

The finding in Equation 16 is that accumulating scalars in one compartment (up or down) instead of two compartments suffice to estimate $\overline{w'c'}$. This assertion will be explored using simulations from measured high-frequency velocity and scalar concentration time series. Once again, some deviations from basic REA approximations may be absorbed by coefficients α_+ and α_- as was done with β. That is, the adjusted 1C-REA can be expressed as

$$\overline{w'c'} = \alpha_+\left[\frac{\sigma_w}{\overline{w^+}}\right]\sigma_w(\overline{c^+}) = \alpha_-\left[\frac{\sigma_w}{\overline{w^-}}\right]\sigma_w(\overline{c^-}). \tag{17}$$

A number of assumptions must now be pointed out regarding the origin of these coefficients α_+ and α_-. Defining $E(.)$ as the ensemble expectation operation, linear regression analysis between x and y necessitates that

$$E(y|x) = R_{xy}x, \tag{18}$$

where $E(y|x)$ is the expectation that y occurs for a known x. Evaluating these expectations at $\overline{w^+}/\sigma_w$ and $\overline{w^-}/\sigma_w$ yields

$$\frac{1}{\sigma_c}\overline{c^+} = E\left(\left(c'/\sigma_c\right)\middle|\left(\overline{w^+}/\sigma_w\right)\right) = \frac{1}{\sigma_w}R_{wc}\overline{w^+}; \tag{19}$$

$$\frac{1}{\sigma_c}\overline{c^-} = E\left(\left(c'/\sigma_c\right)\middle|\left(\overline{w^-}/\sigma_w\right)\right) = \frac{1}{\sigma_w}R_{wc}\overline{w^-}. \tag{20}$$

Stated differently, upon assuming the R_{wc} in Equation 2 is well defined and that time and ensemble-averaging converge, the following symmetries must hold:

$$\frac{E\left(c'/\sigma_c|\overline{w^+}/\sigma_w\right)}{\overline{w^+}/\sigma_w} = \frac{E\left(c'/\sigma_c|\overline{w^-}/\sigma_w\right)}{\overline{w^-}/\sigma_w} = R_{wc}. \tag{21}$$

Moreover, the coefficients α can be interpreted as deviations between time and ensemble-averaged estimates so that

$$\alpha_+ = \frac{E\left(c'/\sigma_c|\overline{w^+}/\sigma_w\right)}{\overline{c^+}/\sigma_c}; \alpha_- = \frac{E\left(c'/\sigma_c|\overline{w^-}/\sigma_w\right)}{\overline{c^-}/\sigma_c}. \tag{22}$$

To recap, Figure 1 presents a sample $w' - c'$ 30-min run for $c' = T'$ (air temperature fluctuations) along with the various estimations of the slope (R_{wc}) for the regression problem $y = R_{wc}x$. The large closed (green) dot associated with updrafts is determined from $\overline{w^+}/\sigma_w$ and $\overline{T^+}/\sigma_T$. Likewise, the large (green) dot associated with downdrafts is determined from $\overline{w^-}/\sigma_w$ and $\overline{T^-}/\sigma_T$. The slope connecting these two points is labeled as the conventional REA or two-compartment REA slope. The one-compartment REA requires that the regression slope passes through the origin and thus uses only one of these two points in the slope (or R_{wc}) estimation: $\overline{w^-}/\sigma_w$ and $\overline{T^-}/\sigma_T$ (labeled as REA minus slope) or $\overline{w^+}/\sigma_w$ and $\overline{T^+}/\sigma_T$ (labeled as REA plus slope). The agreement between all these slope estimates and R_{wc} appears acceptable for this run. Whether these approximations apply to other runs is explored using similar simulations on sampled w', longitudinal velocity $\left(c' = u'\right)$, and air temperature $\left(c' = T'\right)$ across multiple atmospheric stability conditions and surfaces.

3. Data Sets

Sonic anemometry measurements conducted over an ice sheet (in 1993–1994), a dry lake bed (in 1993), a grass field (in 1997), a pine forest (in 1996–1999), a hardwood forest (in 1996), and a deep lake (in 2006) were used to compare the two-compartment and one compartment REA approaches against EC estimates for heat and momentum turbulent fluxes across a wide range of atmospheric stability conditions. The ice sheet runs ($n = 56$) were sampled at 20.8 Hz and collected over the Nansen ice sheet in Antarctica at $z = 10$ m (Cava et al., 2001, 2012). The bare soil runs ($n = 19$) were sampled above a dry lake bed (Owen's Lake, California, USA) at 10 Hz and collected at variable heights ranging from $z = 2$–3 m (Albertson et al., 1995; Chu et al., 1996). The grass site runs ($n = 127$) were sampled at 56 Hz in a large forest clearing at $z = 5.2$ m (grass height about 1 m) within the Duke Forest near Durham, North Carolina (Allouche et al., 2021; G. Katul, Hsieh, & Sigmon, 1997). The pine forest ($n = 130$) and hardwood forest ($n = 180$) sites, also situated within the Blackwood division of the Duke Forest, sampled velocity and temperature at 10 Hz within the roughness sublayer (near the canopy top) across different leaf area index (LAI) values (Cava et al., 2012; G. Katul, Hsieh, Kuhn, et al., 1997). For the hardwood forest site, additional data were collected ($n = 352$) that included runs at multiple levels within the canopy during a seed dispersal experiment (Nathan & Katul, 2005; Nathan et al., 2002). These data, collected in 2001–2002, included runs at low (LAI = 1) and high (LAI = 5) values. Finally, data ($n = 7{,}752$) measured over Lake Geneva, Switzerland, were sampled at four levels ($z = 1.65$, 2.30, 2.95, and 3.60 m, $n = 1{,}938$ at each level) above the surface at a frequency of 20 Hz (Bou-Zeid et al., 2008; Li et al., 2018; Vercauteren et al., 2008). In total, $n = 8{,}589$ runs are used in this comparison each for heat and momentum fluxes. For near-neutral conditions, the sensible heat flux is small whereas the temperature variance remains large. Thus, these near-neutral runs are opportune to explore the behavior of the REA for small correlation coefficients, which may be anticipated for some trace gases.

4. Results and Discussion

The results and discussion are structured as follows: First, an assessment of the deviation between Λ derived from $I(w', c')$ and R_{wc} is conducted for momentum and heat and across all the sites. This comparison seeks to quantify how non-Gaussianity in the empirical $JPDF(w', c')$ impacts the linearity assumptions needed in Equation 18. After completing this assessment, the fourth-order CEM in Equation 10 is used to evaluate how non-Gaussianity in the $JPDF(w', c')$ directly impacts the sought parameter β and its variability across sites. Last, 1C- and 2C-REA calculations are compared against eddy-covariance-based heat and momentum flux estimates across all the sites and atmospheric stability conditions to evaluate the feasibility and generality of the 1C-REA approach.

4.1. Mutual Information and Linear Correlation Measures

Figure 2a compares the Λ (Equation 9) derived from $I(w', c')$ and R_{wc}. As noted in prior studies (Tsonis, 2001), $|\Lambda| \geq |Rwc|$ for almost all the runs whether it be for momentum $(c' = u')$ or heat $(c' = T')$ fluxes. More association between w' and c' exists in all the turbulence records compared to predictions offered by $|R_{wc}|$, especially for small $|R_{wc}| < 0.1$. However, for $|R_{wc}| > 0.3$, Λ and $|R_{wc}|$ track each other (but they are not identical) suggesting that the $JPDF(w', c')$ may be approximated as quasi-Gaussian (but not exactly Gaussian). A direct implication of this result is that M_{40} may be proportional to M_{31}/M_{11} (instead of equal as is the case for Gaussian) and β_{CEM} is an acceptable descriptor of β. Thus, β is explored next with a focus on how statistical non-linearities encoded in the $JPDF(w', c')$ deviations from Gaussian impact Equation 18. The impact of such non-linearities may also be foreshadowed in Figure 1. For the run studied in Figure 1, the expectations of T'/σ_T given binned values of w'/σ_w are computed and presented. These calculations show that in the vicinity of the origin, the $E(T'/\sigma_T | w'/\sigma_w)$ is well approximated by both—the 2C-and 1C- REA slopes as earlier noted. This finding alone hints that a CEM approximation to $JPDF(w', c')$ that models deviations from Gaussian distribution with few cumulants (up to four here) may suffice to assess such effects on β.

Furthermore, the difference in momentum and heat fluxes (and other scalar fluxes such as carbon dioxide and water, checked, but not shown) when they are calculated using a linear regression as opposed to a more general nonlinear measure is attributed to the presence of non linearity in flux transport mechanisms (Chowdhuri et al., 2020). In turn, this level of non linearity can be explained by the difference of flow organization by turbulent coherent structures associated with momentum, heat and scalar fluxes. Further reasoning is beyond the scope of this work, but something we will explore in future research.

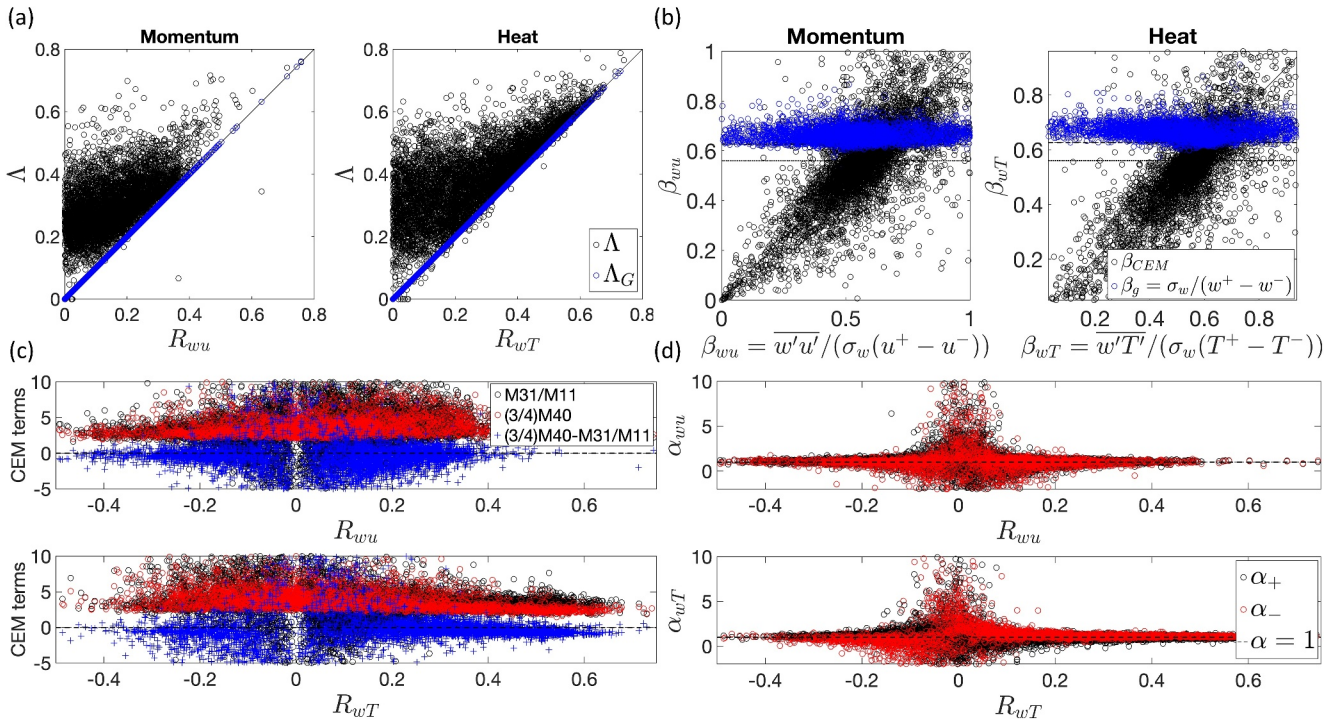

Figure 2. Using all the data sets: (a) Comparison between a linear correlation coefficient against a nonlinear measure of correlation from information theory for momentum (left panel) and heat (right panel). The linear correlation coefficient R_{wc} is plotted on the x axis against the nonlinear estimation of the correlation coefficient Λ on the y axis obtained using mutual information content. The blue circles on the (black) one-to-one line show that the nonlinear measure becomes identical to the linear estimate when using a Gaussian $JPDF(w', c')$. (b) Comparison of β estimations. The x axis plots the theoretical definition of β for the relaxed eddy accumulation method as defined by Equation 1. The y axis plots the β_{CEM} as defined by Equation 10 (black circles). The blue circles show the computed value of β_g from data as given by Equation 7 under Gaussian assumption. The dashed black line shows $\beta_g = \sqrt{(2\pi)}/4$. The dotted black line shows $\beta_{CEM} = 0.56$ when Equation 11 is satisfied. (c) Examining the equality of the two cumulant expansion method terms on the two sides of Equation 11. The x axis shows R_{wc} and the y axis shows the terms $M31/M11$ using black circles and $(3/4)M40$ using red circles. The blue + markers show the residual between the two terms and the dashed line shows the zero line for reference. (d) Comparison of α estimations for the 1C-REA approach. The x axis plots R_{wc} and the y axis plots α_+ and α_- as defined by Equation 22. The black dashed line plots $\alpha = 1$ for reference.

4.2. CEM Approximations to the $JPDF(w', c')$ and β Variations

Motivated by the prior findings, the extent to which these non-linearities and concomitant associations derived from $I(w', c')$ impact the constancy and numerical values of β are analytically addressed using the CEM approximation to the $JPDF(w', c')$. Figure 2b compares the β predictions from CEM (labeled β_{CEM}), the Gaussian distribution for w' (labeled β_g), the $\beta = 0.56$ (derived from Equation 11) and β derived from the statistics of w' only (as in the original REA) for momentum and heat fluxes at all sites. The β_{CEM} reproduces best the empirically derived $\beta = \overline{w'c'}\left[\sigma_w\left(\overline{c^+} - \overline{c^-}\right)\right]^{-1}$ when using measured $\overline{w'c'}$ for both momentum and heat. It is also noted that the β defined by Equation 1 does vary around a mean value ≈ 0.56, although there is a larger standard deviation. The agreement in Figure 2b lends confidence that the CEM approximation introduced here and elsewhere (G. Katul et al., 2018; Milne et al., 1999) captures the salient features of the non-Gaussian $JPDF(w', c')$ and their impact on β for both heat and momentum. To be clear, β_{CEM} requires high-order velocity-scalar covariances that cannot be determined in REA formulation and is only used here for diagnostic purposes.

Figure 2c explores the dominant terms in β_{CEM} that introduce variability in measured β. The first term is related to the intermittency of w' only (i.e., $(3/4)M_{40}$) while the second is related to high-order moments of scalar-velocity interaction asymmetry (i.e., M_{31}/R_{wc}). For high R_{wc}, the imbalance between these two terms is small as predicted from a quasi-Gaussian $JPDF(w', c')$ whereas for small R_{wc}, the term M_{31}/M_{11} exhibits high "volatility." This volatility in M_{31}/M_{11} can be foreshadowed because $(3/4)M_{40}$ is insensitive to R_{wc} and remains finite whereas

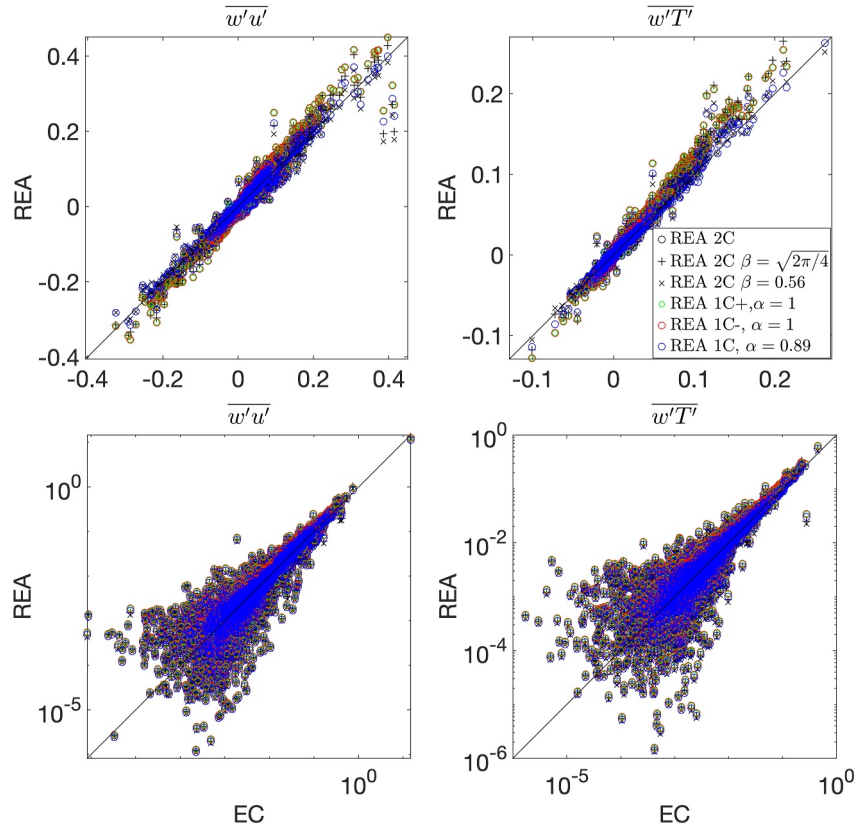

Figure 3. The top two panels show comparisons of $\overline{w'c'}$ (left: momentum $\left(\mathrm{m^2\ s^{-2}}\right)$; right: heat $\left(\mathrm{K\ m\ s^{-1}}\right)$) estimated using the eddy covariance method on the x axis and the relaxed eddy accumulation (REA) method on the y axis. The black circles show the standard two-compartment REA estimation using Equation 4, while the black + and x markers show the simplified two-compartment REA estimation using a fixed $\beta = \sqrt{2\pi/4}$ and 0.56 respectively using Equation 1. The green (positive side) and the red (negative side) circles show the proposed one-compartment REA estimations, which match each other. The blue markers show the one-sided (same for plus or minus) estimation with a modified $\alpha = 0.89$ instead of unity. This α modification from unity is identical to β adjustments to accommodate non-Gaussian statistics (i.e., $\beta_{CEM}/\beta_g = 0.56/0.63 = 0.89$). The black line represents the one-to-one line. The bottom panels show the same data, just (using absolute values of the fluxes) on the logarithmic axes for visual clarity.

M_{31}/M_{11} becomes ill defined as $|R_{wc}| \to 0$ given that both M_{11} and M_{31} become small making their ratio numerically ill-determined. These findings hold for both momentum and heat transport.

4.3. The Performance of the One-Compartment REA

Analogous to the parameter β, we now explore the variation of the parameter α for one compartment REA beginning with Equation 22. Figure 2d shows that, in analogy to β, α_+ and α_- are equal and near unity for high R_{wc} for $c' = u'$ and $c' = T'$. However, for $|R_{wc}| < 0.15$, the scatter is large just as found for β. To elaborate on the practical utility of the REA methods, a comparison between measured $\overline{w'c'}$ (i.e., eddy-covariance based) and REA estimated fluxes is carried out in Figure 3. Agreement between 1C- and 2C- REA momentum and heat fluxes with eddy-covariance (EC) based measurements is acceptable even at low flux values, for positive $\overline{w'u'}$, and negative $\overline{w'T'}$. While the relative errors appear large in the flux comparisons at small fluxes, the absolute error is small. The scatter around the one-to-one line at small fluxes in this comparison is also suggestive that these deviations may be random and thus "averaged" out if sufficient runs at small flux values are sampled by 1C- or 2C- REA. Note that at the low values of R_{wu}, there is more nonlinear correlation between w' and u' or T' (more departure from a Gaussian JPDF) as encoded in the Λ parameter given by Equation 9. At higher correlation values, the JPDF tends to be more Gaussian and therefore the linear correlation measures are more robust and α or

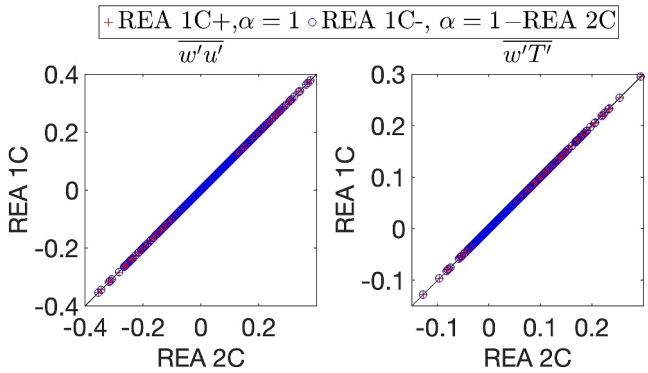

Figure 4. Comparing the 2C-against 1C-relaxed eddy accumulation. The one-to-one line is also shown.

β are closer to their linear estimations. In the next section, it is shown that the 1C- and 2C- REA flux calculations are virtually indistinguishable even at small fluxes.

Figure 4 shows the comparison between the 1C-REA and the 2C-REA when setting $\alpha = 1$. These calculations assume β is given by $\beta_g = \sigma_w/(\overline{w^+} - \overline{w^-})$. A one-to-one agreement implies that any fractional adjustment in β corresponds to an equal fractional adjustment in α (from unity). For example, setting $\beta = 0.56$ is equivalent to setting $\alpha = (0.56/\beta_g) = 0.89$ for $\beta_g = \sqrt{2\pi}/4$. The root mean square percent error between the standard two-compartment REA with $\beta = \sqrt{(2\pi)}/4 \approx 0.63$ and the proposed one-compartment REA was found to be 3.28% for momentum flux and 2.47% for sensible heat flux for all data sets used in this study.

5. Conclusions

It is demonstrated that the conventional or 2C-REA approach to compute turbulent fluxes can be simplified to a one-compartment approach (either an updraft or a downdraft compartment) without loss of generality. This finding can immediately expand the operational utility of REA in future field campaigns. This conclusion appears robust to the findings that the association between w' and c' deviates from predictions using a linear correlation coefficient R_{wc}, especially at low $|R_{wc} \leq 0.15|$. When the association between w' and c' is computed from a mutual information measure, deviations between linear and non-linear correlations can be traced back to deviations between the empirically derived $JPDF(w', c')$ and a Gaussian approximation to it. A fourth-order CEM of the $JPDF(w', c')$ capturing deviations in asymmetry and intermittency from a Gaussian shape is shown to be sufficient to reproduce the variability in the 2C-REA coefficient β when inferred using the conventional formulation. The non-constant β arises because of an imbalance between two dominant cumulants: M_{40} and M_{31}/M_{11}, where $M_{ij} = \overline{w'^i c'^j}/(\sigma_w^i \sigma_c^j)$. The M_{40} depends on the intermittent behavior of w' only whereas M_{31}/M_{11} can depend on scalar statistics and their interaction with w'. That these two cumulants are roughly in balance across such a wide range of surfaces and atmospheric stability conditions for $|R_{wc}| > 0.15$ points to surprisingly high coordination between intermittency in w' and asymmetry captured by M_{31}. For high $|R_{wc}| > 0.15$, a quasi-Gaussian $JPDF(w', c')$ alone explains the high coordination between M_{40} and M_{31}/M_{11} as well as the near-constant β_{CEM}. Returning to the relevance of this finding to the REA approach across a wide range of surface cover types and atmospheric stability conditions, the near-cancellation of these two terms results in $\beta = 0.56$, a constant. Variability in β at low $|R_{wc}|$ can thus be explained by the fact that both M_{31} and M_{11} become small making their ratio numerically indeterminate. However, for small turbulent fluxes, the deviations between REA and eddy-covariance-based approaches appear random whether a 1C- or a 2C- REA formulation is employed. This finding is of significance because it implies that such errors can be averaged out with sufficient sampling, a finding that was also reported in a recent study (Dias et al., 2023). Thus, it can be surmised that a one-compartment REA is, in principle, feasible for turbulent flux measurements even when the fluxes are small. Building the apparatus for its field implementation is a topic left for the future.

To summarize, we have investigated the assumptions behind the standard REA technique and explored the conditions under which the two compartment REA framework can be approximated with a one compartment REA. We have also demonstrated that under the assumption of linear correlation between vertical velocity fluctuations and scalar concentration fluctuations, the 2 and 1C REA are virtually identical. Nevertheless, under these conditions, the β parameter involved in the REA flux calculation requires high-frequency scalar fluctuation measurements. However, the assumption of a Gaussian joint pdf of velocity and scalar concentration fluctuations can be invoked to simplify this measurement that can either use only high-frequency vertical velocity fluctuations using sonic anemometer data or a constant β. Beyond these scenarios, we refrain from commenting on the details of hardware and construction of the 1C-REA apparatus as it is beyond the scope of this work. To conclude, these findings establish the framework for simplifying the standard REA technique since measuring one compartment could be potentially more operationally convenient than two compartments.

Data Availability Statement

No new data were collected for the purposes of this study. The ice sheet data are available through Cava et al. (2001, 2012). The bare soil data are available through Albertson et al. (1995), Chu et al. (1996). The grass site data are available through G. Katul, Hsieh, and Sigmon (1997), and Allouche et al. (2021). The pine forest data and the hardwood forest data are available through Cava et al. (2012), G. Katul, Hsieh, and Kuhn et al. (1997). The hardwood forest data from the seed dispersal experiment are available through Nathan et al. (2002) and Nathan and Katul (2005). Finally, the Lake Geneva data are available through Bou-Zeid et al. (2008), Vercauteren et al. (2008), and Li et al. (2018).

Acknowledgments

TB is supported by the US National Science Foundation (*NSF-AGS-PDM-2146520*, *NSF-OISE-2114740*, *NSF-CPS-2209695*, *NSF-ECO-CBET-2318718*, and *NSF-DMS-2335847*), the University of California Office of the President (UCOP-LFR-20-653572), NASA (*80NSSC22K1911*), and the United States Department of Agriculture (*NIFA 2021-67022-35908*, and *USDA-20-CR-11242306-072*). GK is supported by the US National Science Foundation (*NSF-AGS-2028633*) and the Department of Energy (*DE-SC0022072*). NLD is supported by CNPq's (Brazil's National Research Council) Research Scholarship (*305903/2021-7*). EZ and EBZ are supported by the US National Science Foundation (*NSF-AGS-2128345*) and the High Meadows Environmental Institute of Princeton University.

References

Albertson, J. D., Parlange, M. B., Katul, G. G., Chu, C.-R., Stricker, H., & Tyler, S. (1995). Sensible heat flux from arid regions: A simple flux-variance method. *Water Resources Research*, *31*(4), 969–973. https://doi.org/10.1029/94wr02978

Allouche, M., Katul, G. G., Fuentes, J. D., & Bou-Zeid, E. (2021). Probability law of turbulent kinetic energy in the atmospheric surface layer. *Physical Review Fluids*, *6*(7), 074601. https://doi.org/10.1103/physrevfluids.6.074601

Ammann, C., & Meixner, F. (2002). Stability dependence of the relaxed eddy accumulation coefficient for various scalar quantities. *Journal of Geophysical Research*, *107*(D8), 4071. https://doi.org/10.1029/2001JD000649

Andreas, E. L., Hill, R. J., Gosz, J. R., Moore, D. I., Otto, W. D., & Sarma, A. D. (1998). Stability dependence of the eddy-accumulation coefficients for momentum and scalars. *Boundary-Layer Meteorology*, *86*(3), 409–420. https://doi.org/10.1023/a:1000625502550

Arnts, R. R., Mowry, F. L., & Hampton, G. A. (2013). A high-frequency response relaxed eddy accumulation flux measurement system for sampling short-lived biogenic volatile organic compounds. *Journal of Geophysical Research: Atmospheres*, *118*(10), 4860–4873. https://doi.org/10.1002/jgrd.50215

Baker, B., Guenther, A., Greenberg, J., Goldstein, A., & Fall, R. (1999). Canopy fluxes of 2-methyl-3-buten-2-ol over a ponderosa pine forest by relaxed eddy accumulation: Field data and model comparison. *Journal of Geophysical Research*, *104*(D21), 26107–26114. https://doi.org/10.1029/1999jd900749

Baker, J., Norman, J., & Bland, W. (1992). Field-scale application of flux measurement by conditional sampling. *Agricultural and Forest Meteorology*, *62*(1–2), 31–52. https://doi.org/10.1016/0168-1923(92)90004-n

Banerjee, T., De Roo, F., & Mauder, M. (2017). Connecting the failure of K theory inside and above vegetation canopies and ejection-sweep cycles by a large-eddy simulation. *Journal of Applied Meteorology and Climatology*, *56*(12), 3119–3131. https://doi.org/10.1175/jamc-d-16-0363.1

Beverland, I., Oneill, D., Scott, S., & Moncrieff, J. (1996). Design, construction and operation of flux measurement systems using the conditional sampling technique. *Atmospheric Environment*, *30*(18), 3209–3220. https://doi.org/10.1016/1352-2310(96)00010-6

Bou-Zeid, E., Vercauteren, N., Parlange, M. B., & Meneveau, C. (2008). Scale dependence of subgrid-scale model coefficients: An a priori study. *Physics of Fluids*, *20*(11), 115106. https://doi.org/10.1063/1.2992192

Bowling, D., Turnipseed, A., Delany, A., Baldocchi, D., Greenberg, J., & Monson, R. (1998). The use of relaxed eddy accumulation to measure biosphere-atmosphere exchange of isoprene and other biological trace gases. *Oecologia*, *116*(3), 306–315. https://doi.org/10.1007/s004420050592

Brut, A., Legain, D., Durand, P., & Laville, P. (2004). A relaxed eddy accumulator for surface flux measurements on ground-based platforms and aboard research vessels. *Journal of Atmospheric and Oceanic Technology*, *21*(3), 411–427. https://doi.org/10.1175/1520-0426(2004)021<0411:areafs>2.0.co;2

Businger, J. A., & Oncley, S. P. (1990). Flux measurement with conditional sampling. *Journal of Atmospheric and Oceanic Technology*, *7*(2), 349–352. https://doi.org/10.1175/1520-0426(1990)007<0349:fmwcs>2.0.co;2

Cava, D., Giostra, U., & Tagliazucca, M. (2001). Spectral maxima in a perturbed stable boundary layer. *Boundary-Layer Meteorology*, *100*(3), 421–437. https://doi.org/10.1023/a:1019219117439

Cava, D., Katul, G., Scrimieri, A., Poggi, D., Cescatti, A., & Giostra, U. (2006). Buoyancy and the sensible heat flux budget within dense canopies. *Boundary-Layer Meteorology*, *118*(1), 217–240. https://doi.org/10.1007/s10546-005-4736-1

Cava, D., Katul, G. G., Molini, A., & Elefante, C. (2012). The role of surface characteristics on intermittency and zero-crossing properties of atmospheric turbulence. *Journal of Geophysical Research*, *117*(D1), D01104. https://doi.org/10.1029/2011JD016167

Chowdhuri, S., Prabhakaran, T., & Banerjee, T. (2020). Persistence behavior of heat and momentum fluxes in convective surface layer turbulence. *Physics of Fluids*, *32*(11), 115107. https://doi.org/10.1063/5.0027168

Chu, C. R., Parlange, M. B., Katul, G. G., & Albertson, J. D. (1996). Probability density functions of turbulent velocity and temperature in the atmospheric surface layer. *Water Resources Research*, *32*(6), 1681–1688. https://doi.org/10.1029/96wr00287

Dabberdt, W., Lenschow, D., Horst, T., Zimmerman, P., Oncley, S., & Delany, A. (1993). Atmosphere-surface exchange measurements. *Science*, *260*(5113), 1472–1481. https://doi.org/10.1126/science.260.5113.1472

Darmais, S., Dutaur, L., Larsen, B., Cieslik, S., Luchetta, L., Simon, V., & Torres, L. (2000). Emission fluxes of VOC by orange trees determined by both relaxed eddy accumulation and vertical gradient approaches. *Chemosphere-Global Change Science*, *2*(1), 47–56. https://doi.org/10.1016/s1465-9972(99)00050-1

Denmead, O. (2008). Approaches to measuring fluxes of methane and nitrous oxide between landscapes and the atmosphere. *Plant and Soil*, *309*(1–2), 5–24. https://doi.org/10.1007/s11104-008-9599-z

Desjardins, R. (1977). Description and evaluation of a sensible heat flux detector. *Boundary-Layer Meteorology*, *11*(2), 147–154. https://doi.org/10.1007/bf02166801

Desjardins, R., Pattey, E., Smith, W., Worth, D., Grant, B., Srinivasan, R., et al. (2010). Multiscale estimates of N_2O emissions from agricultural lands. *Agricultural and Forest Meteorology*, *150*(6), 817–824. https://doi.org/10.1016/j.agrformet.2009.09.001

Dias, N. L., Toro, I. M. C., Dias-Júnior, C. Q., Mortarini, L., & Brondani, D. (2023). The relaxed eddy accumulation method over the Amazon forest: The importance of flux strength on individual and aggregated flux estimates. *Boundary-Layer Meteorology*, *189*(1), 139–161. https://doi.org/10.1007/s10546-023-00829-7

Fer, I., McPhee, M. G., & Sirevaag, A. (2004). Conditional statistics of the Reynolds stress in the under-ice boundary layer. *Geophysical Research Letters*, *31*(15), L15311. https://doi.org/10.1029/2004GL020475

Francone, C., Katul, G. G., Cassardo, C., & Richiardone, R. (2012). Turbulent transport efficiency and the ejection-sweep motion for momentum and heat on sloping terrain covered with vineyards. *Agricultural and Forest Meteorology*, *162*, 98–107. https://doi.org/10.1016/j.agrformet.2012.04.012

Gaman, A., Rannik, Ü., Aalto, P., Pohja, T., Siivola, E., Kulmala, M., & Vesala, T. (2004). Relaxed eddy accumulation system for size-resolved aerosol particle flux measurements. *Journal of Atmospheric and Oceanic Technology*, *21*(6), 933–943. https://doi.org/10.1175/1520-0426(2004)021<0933:reasfs>2.0.co;2

Gao, W. (1995). The vertical change of coefficient β used in the relaxed eddy accumulation method for flux measurement above and within a forest canopy. *Atmospheric Environment*, *29*(17), 2339–2347. https://doi.org/10.1016/1352-2310(95)00147-q

Grelle, A., & Keck, H. (2021). Affordable relaxed eddy accumulation system to measure fluxes of H_2O, CO_2, CH_4 and N_2O from ecosystems. *Agricultural and Forest Meteorology*, *307*, 108514. https://doi.org/10.1016/j.agrformet.2021.108514

Grönholm, T., Aalto, P. P., Hiltunen, V. J., Rannik, Ü., Rinne, J., Laakso, L., et al. (2007). Measurements of aerosol particle dry deposition velocity using the relaxed eddy accumulation technique. *Tellus B: Chemical and Physical Meteorology*, *59*(3), 381–386. https://doi.org/10.3402/tellusb.v59i3.16998

Heisel, M., Katul, G. G., Chamecki, M., & Guala, M. (2020). Velocity asymmetry and turbulent transport closure in smooth-and rough-wall boundary layers. *Physical Review Fluids*, *5*(10), 104605. https://doi.org/10.1103/physrevfluids.5.104605

Held, A., Patton, E., Rizzo, L., Smith, J., Turnipseed, A., & Guenther, A. (2008). Relaxed eddy accumulation simulations of aerosol number fluxes and potential proxy scalars. *Boundary-Layer Meteorology*, *129*(3), 451–468. https://doi.org/10.1007/s10546-008-9327-5

Hensen, A., Nemitz, E., Flynn, M., Blatter, A., Jones, S., Sørensen, L. L., et al. (2009). Inter-comparison of ammonia fluxes obtained using the relaxed eddy accumulation technique. *Biogeosciences*, *6*(11), 2575–2588. https://doi.org/10.5194/bg-6-2575-2009

Hornsby, K., Flynn, M., Dorsey, J., Gallagher, M., Chance, R., Jones, C., & Carpenter, L. (2009). A relaxed eddy accumulation (REA)-GC/MS system for the determination of halocarbon fluxes. *Atmospheric Measurement Techniques*, *2*(2), 437–448. https://doi.org/10.5194/amt-2-437-2009

Katul, G., Albertson, J., Chu, C.-R., Parlange, M., Stricker, H., & Tyler, S. (1994). Sensible and latent heat flux predictions using conditional sampling methods. *Water Resources Research*, *30*(11), 3053–3059. https://doi.org/10.1029/94wr01673

Katul, G., Hsieh, C.-I., Kuhn, G., Ellsworth, D., & Nie, D. (1997). Turbulent eddy motion at the forest-atmosphere interface. *Journal of Geophysical Research*, *102*(D12), 13409–13421. https://doi.org/10.1029/97jd00777

Katul, G., Hsieh, C.-I., & Sigmon, J. (1997). Energy-inertial scale interactions for velocity and temperature in the unstable atmospheric surface layer. *Boundary-Layer Meteorology*, *82*(1), 49–80. https://doi.org/10.1023/a:1000178707511

Katul, G., Peltola, O., Grönholm, T., Launiainen, S., Mammarella, I., & Vesala, T. (2018). Ejective and sweeping motions above a peatland and their role in relaxed-eddy-accumulation measurements and turbulent transport modelling. *Boundary-Layer Meteorology*, *169*(2), 163–184. https://doi.org/10.1007/s10546-018-0372-4

Katul, G., Poggi, D., Cava, D., & Finnigan, J. (2006). The relative importance of ejections and sweeps to momentum transfer in the atmospheric boundary layer. *Boundary-Layer Meteorology*, *120*(3), 367–375. https://doi.org/10.1007/s10546-006-9064-6

Katul, G. G., Finkelstein, P. L., Clarke, J. F., & Ellestad, T. G. (1996). An investigation of the conditional sampling method used to estimate fluxes of active, reactive, and passive scalars. *Journal of Applied Meteorology and Climatology*, *35*(10), 1835–1845. https://doi.org/10.1175/1520-0450(1996)035<1835:aiotcs>2.0.co;2

Lemaire, B. J., Noss, C., & Lorke, A. (2017). Toward relaxed eddy accumulation measurements of sediment-water exchange in aquatic ecosystems. *Geophysical Research Letters*, *44*(17), 8901–8909. https://doi.org/10.1002/2017gl074625

Li, Q., Bou-Zeid, E., Vercauteren, N., & Parlange, M. (2018). Signatures of air–wave interactions over a large lake. *Boundary-Layer Meteorology*, *167*(3), 445–468. https://doi.org/10.1007/s10546-017-0329-z

McInnes, K. J., & Heilman, J. L. (2005). Relaxed eddy accumulation. *Micrometeorology in Agricultural Systems*, *47*, 437–453. https://doi.org/10.2134/agronmonogr47.c19

Meskhidze, N., Royalty, T. M., Phillips, B., Dawson, K. W., Petters, M. D., Reed, R., et al. (2018). Continuous flow hygroscopicity-resolved relaxed eddy accumulation (Hy-Res REA) method of measuring size-resolved sodium chloride particle fluxes. *Aerosol Science and Technology*, *52*(4), 433–450. https://doi.org/10.1080/02786826.2017.1423174

Meyers, T., Luke, W., & Meisinger, J. (2006). Fluxes of ammonia and sulfate over maize using relaxed eddy accumulation. *Agricultural and Forest Meteorology*, *136*(3–4), 203–213. https://doi.org/10.1016/j.agrformet.2004.10.005

Milne, R., Beverland, I., Hargreaves, K., & Moncrieff, J. (1999). Variation of the β coefficient in the relaxed eddy accumulation method. *Boundary-Layer Meteorology*, *93*(2), 211–225. https://doi.org/10.1023/a:1002061514948

Mochizuki, T., Tani, A., Takahashi, Y., Saigusa, N., & Ueyama, M. (2014). Long-term measurement of terpenoid flux above a Larix kaempferi forest using a relaxed eddy accumulation method. *Atmospheric Environment*, *83*, 53–61. https://doi.org/10.1016/j.atmosenv.2013.10.054

Monin, A., & Yaglom, A. (1971). *Statistical fluid mechanics: Mechanics of turbulence* (Vol. 1). MIT Press.

Nakagawa, H., & Nezu, I. (1977). Prediction of the contributions to the Reynolds stress from bursting events in open-channel flows. *Journal of Fluid Mechanics*, *80*(1), 99–128. https://doi.org/10.1017/s0022112077001554

Nathan, R., & Katul, G. G. (2005). Foliage shedding in deciduous forests lifts up long-distance seed dispersal by wind. *Proceedings of the National Academy of Sciences*, *102*(23), 8251–8256. https://doi.org/10.1073/pnas.0503048102

Nathan, R., Katul, G. G., Horn, H. S., Thomas, S. M., Oren, R., Avissar, R., et al. (2002). Mechanisms of long-distance dispersal of seeds by wind. *Nature*, *418*(6896), 409–413. https://doi.org/10.1038/nature00844

Nie, D., Kleindienst, T., Arnts, R., & Sickles, J. (1995). The design and testing of a relaxed eddy accumulation system. *Journal of Geophysical Research*, *100*(D6), 11415–11423. https://doi.org/10.1029/95jd01042

Olofsson, M., Ek-Olausson, B., Ljungström, E., & Langer, S. (2003). Flux of organic compounds from grass measured by relaxed eddy accumulation technique. *Journal of Environmental Monitoring*, *5*(6), 963–970. https://doi.org/10.1039/b303329e

Oncley, S. P., Delany, A. C., Horst, T. W., & Tans, P. P. (1993). Verification of flux measurement using relaxed eddy accumulation. Atmospheric Environment. Part A. *General Topics*, *27*(15), 2417–2426. https://doi.org/10.1016/0960-1686(93)90409-r

Paluš, M., & Novotná, D. (1994). Testing for nonlinearity in weather records. *Physics Letters A*, *193*(1), 67–74. https://doi.org/10.1016/0375-9601(94)91002-2

Pattey, E., Cessna, A., Desjardins, R., Ken, L., Rochette, P., St-Amour, G., et al. (1995). Herbicides volatilization measured by the relaxed eddy-accumulation technique using two trapping media. *Agricultural and Forest Meteorology*, *76*(3–4), 201–220. https://doi.org/10.1016/0168-1923(95)02225-m

Pattey, E., Desjardins, R., & Rochette, P. (1993). Accuracy of the relaxed eddy-accumulation technique evaluated using CO_2 flux measurements. *Boundary-Layer Meteorology*, *66*(4), 341–355. https://doi.org/10.1007/bf00712728

Pattey, E., Desjardins, R., Westberg, H., Lamb, B., & Zhu, T. (1999). Measurement of isoprene emissions over a black spruce stand using a tower-based relaxed eddy-accumulation system. *Journal of Applied Meteorology and Climatology*, *38*(7), 870–877. https://doi.org/10.1175/1520-0450(1999)038<0870:moieoa>2.0.co;2

Poggi, D., & Katul, G. (2007). The ejection-sweep cycle over bare and forested gentle hills: A laboratory experiment. *Boundary-Layer Meteorology*, *122*(3), 493–515. https://doi.org/10.1007/s10546-006-9117-x

Poggi, D., Katul, G., & Albertson, J. (2004). Momentum transfer and turbulent kinetic energy budgets within a dense model canopy. *Boundary-Layer Meteorology*, *111*(3), 589–614. https://doi.org/10.1023/b:boun.0000016502.52590.af

Pryor, S., Larsen, S. E., Sørensen, L. L., Barthelmie, R. J., Grönholm, T., Kulmala, M., et al. (2007). Particle fluxes over forests: Analyses of flux methods and functional dependencies. *Journal of Geophysical Research*, *112*(D7), D07205. https://doi.org/10.1029/2006JD008066

Raupach, M. (1981). Conditional statistics of Reynolds stress in rough-wall and smooth-wall turbulent boundary layers. *Journal of Fluid Mechanics*, *108*, 363–382. https://doi.org/10.1017/s0022112081002164

Ren, X., Sanders, J., Rajendran, A., Weber, R., Goldstein, A., Pusede, S., et al. (2011). A relaxed eddy accumulation system for measuring vertical fluxes of nitrous acid. *Atmospheric Measurement Techniques*, *4*(10), 2093–2103. https://doi.org/10.5194/amt-4-2093-2011

Rhew, R. C., Deventer, M. J., Turnipseed, A. A., Warneke, C., Ortega, J., Shen, S., et al. (2017). Ethene, propene, butene and isoprene emissions from a ponderosa pine forest measured by relaxed eddy accumulation. *Atmospheric Chemistry and Physics*, *17*(21), 13417–13438. https://doi.org/10.5194/acp-17-13417-2017

Ruppert, J., Thomas, C., & Foken, T. (2006). Scalar similarity for relaxed eddy accumulation methods. *Boundary-Layer Meteorology*, *120*(1), 39–63. https://doi.org/10.1007/s10546-005-9043-3

Sakabe, A., Ueyama, M., Kosugi, Y., Hamotani, K., Hirano, T., & Hirata, R. (2014). Is the empirical coefficient β for the relaxed eddy accumulation method constant? *Journal of Atmospheric Chemistry*, *71*(1), 79–94. https://doi.org/10.1007/s10874-014-9282-0

Sarkar, C., Turnipseed, A., Shertz, S., Karl, T., Potosnak, M., Bai, J., et al. (2020). A portable, low-cost relaxed eddy accumulation (REA) system for quantifying ecosystem-level fluxes of volatile organics. *Atmospheric Environment*, *242*, 117764. https://doi.org/10.1016/j.atmosenv.2020.117764

Schery, S. D., Wasiolek, P. T., Nemetz, B. M., Yarger, F. D., & Whittlestone, S. (1998). Relaxed eddy accumulator for flux measurement of nanometer-size particles. *Aerosol Science and Technology*, *28*(2), 159–172. https://doi.org/10.1080/02786829808965518

Shannon, C. E. (1948). A mathematical theory of communication. *The Bell system technical journal*, *27*(3), 379–423. https://doi.org/10.1002/j.1538-7305.1948.tb01338.x

Tsai, J.-L., Tsuang, B.-J., Kuo, P.-H., Tu, C.-Y., Chen, C.-L., Hsueh, M.-T., et al. (2012). Evaluation of the relaxed eddy accumulation coefficient at various wetland ecosystems. *Atmospheric Environment*, *60*, 336–347. https://doi.org/10.1016/j.atmosenv.2012.06.081

Tsonis, A. (2001). Probing the linearity and nonlinearity in the transitions of the atmospheric circulation. *Nonlinear Processes in Geophysics*, *8*(6), 341–345. https://doi.org/10.5194/npg-8-341-2001

Tsonis, A., Triantafyllou, G., & Elsner, J. (1994). Searching for determinism in observed data: A review of the issues involved. *Nonlinear Processes in Geophysics*, *1*(1), 12–25. https://doi.org/10.5194/npg-1-12-1994

Velentini, R., Greco, S., Seufert, G., Bertin, N., Ciccioli, P., Cecinato, A., et al. (1997). Fluxes of biogenic VOC from Mediterranean vegetation by trap enrichment relaxed eddy accumulation. *Atmospheric Environment*, *31*, 229–238. https://doi.org/10.1016/s1352-2310(97)00085-x

Vercauteren, N., Bou-Zeid, E., Parlange, M. B., Lemmin, U., Huwald, H., Selker, J., & Meneveau, C. (2008). Subgrid-scale dynamics of water vapour, heat, and momentum over a lake. *Boundary-Layer Meteorology*, *128*(2), 205–228. https://doi.org/10.1007/s10546-008-9287-9

von der Heyden, L., Wißdorf, W., Kurtenbach, R., & Kleffmann, J. (2022). A relaxed eddy accumulation (REA) LOPAP system for flux measurements of nitrous acid (HONO). *Atmospheric Measurement Techniques*, *15*(6), 1983–2000. https://doi.org/10.5194/amt-15-1983-2022

Xu, X., Bingemer, H., & Schmidt, U. (2002). The flux of carbonyl sulfide and carbon disulfide between the atmosphere and a spruce forest. *Atmospheric Chemistry and Physics*, *2*(3), 171–181. https://doi.org/10.5194/acp-2-171-2002

Zahn, E., Bou-Zeid, E., & Dias, N. L. (2023). Relaxed Eddy Accumulation outperforms Monin-Obukhov flux models under non-ideal conditions. *Geophysical Research Letters*, *50*(7), e2023GL103099. https://doi.org/10.1029/2023gl103099

Zahn, E., Dias, N. L., Araújo, A., Sá, L. D., Sörgel, M., Trebs, I., et al. (2016). Scalar turbulent behavior in the roughness sublayer of an Amazonian forest. *Atmospheric Chemistry and Physics*, *16*(17), 11349–11366. https://doi.org/10.5194/acp-16-11349-2016

Zemmelink, H., Gieskes, W., Klaassen, W., De Groot, H., De Baar, H., Dacey, J., et al. (2002). Simultaneous use of relaxed eddy accumulation and gradient flux techniques for the measurement of sea-to-air exchange of dimethyl sulphide. *Atmospheric Environment*, *36*(36–37), 5709–5717. https://doi.org/10.1016/s1352-2310(02)00577-0

Zemmelink, H. J., Gieskes, W. W., Klaassen, W., Beukema, W. J., de Groot, H. W., de Baar, H. J., et al. (2004). Relaxed eddy accumulation measurements of the sea-to-air transfer of dimethylsulfide over the northeastern Pacific. *Journal of Geophysical Research*, *109*(C1), 1–10. https://doi.org/10.1029/2002JC001617

Zhang, N., Zhou, X., Bertman, S., Tang, D., Alaghmand, M., Shepson, P., & Carroll, M. (2012). Measurements of ambient HONO concentrations and vertical HONO flux above a northern Michigan forest canopy. *Atmospheric Chemistry and Physics*, *12*(17), 8285–8296. https://doi.org/10.5194/acp-12-8285-2012

Zhu, T., Pattey, E., & Desjardins, R. (2000). Relaxed eddy-accumulation technique for measuring ammonia volatilization. *Environmental Science & Technology*, *34*(1), 199–203. https://doi.org/10.1021/es980928f